# Satellite data analysis and numerical simulation of tropical cyclone formation

Tim Li, Bing Fu, Xuyang Ge, Bin Wang, and Melinda Peng[1]

Department of Meteorology, University of Hawaii, Honolulu, Hawaii, USA

Received 4 September 2003; revised 3 October 2003; accepted 15 October 2003; published 13 November 2003.

[1] Forecast of tropical cyclone (TC) formation has long been a great challenge owing to lack of reliable observations over vast open oceans. Recent satellite products provide a unique opportunity to reveal detailed atmospheric wave structures prior to TC formation. Using the QuikSCAT surface wind and the Tropical Rainfall Measurement Mission Microwave Image data, we document temporal and spatial structures of Rossby wave trains induced by energy dispersion from a pre-existing TC and easterly wave propagation characteristics prior to cyclogenesis in the western North Pacific. Using a baroclinic model, we further simulate cyclogenesis processes associated with the TC energy dispersion and easterly waves. *INDEX TERMS:* 3337 Meteorology and Atmospheric Dynamics: Numerical modeling and data assimilation; 3364 Meteorology and Atmospheric Dynamics: Synoptic-scale meteorology; 3374 Meteorology and Atmospheric Dynamics: Tropical meteorology.
**Citation:** Li, T., B. Fu, X. Ge, B. Wang, and M. Peng, Satellite data analysis and numerical simulation of tropical cyclone formation, *Geophys. Res. Lett.*, *30*(21), 2122, doi:10.1029/2003GL018556, 2003.

## 1. Introduction

[2] The skill of the tropical cyclone (TC) track forecast has been substantially improved in past decades [*Kurihara et al.*, 1995], but the prediction of TC formation is still in an infant stage. Observations show that the western North Pacific (WNP) is the region of most frequent TC formation on the earth. About 40% of the total TCs worldwide are generated in this region each year. Over 80% of the TCs in the WNP form in the intertropical convergence zone (ITCZ)/monsoon trough, where both the large-scale confluent flow and warm ocean surface favor the formation of synoptic-scale disturbances and TCs [*Gray*, 1968].

[3] *Ritchie and Holland* [1999] identified three types of environmental flow regimes associated with TC genesis in the WNP: the monsoon shear line, the monsoon confluence region, and the monsoon gyre. While theses large-scale flow patterns no doubt play important roles in providing background stages for tropical storm development, it is synoptic-scale waves/disturbances that often serve as precursor perturbations for triggering individual cyclogenesis events. Thus TC formation depends crucially on the development of synoptic-scale perturbations and their interactions with large-scale background flows.

[4] From a synoptic-scale perturbation perspective, two processes are particularly relevant to WNP cyclogenesis. The first is associated with Rossby wave energy dispersion from a pre-existing TC [*Frank*, 1982; *Davidson and Hendon*, 1989; *Briegel and Frank*, 1997; *Ritchie and Holland*, 1997]. A mature TC is subject to Rossby wave energy dispersion due to change of the Coriolis force with latitude [e.g., *Anthes*, 1982; *Flierl*, 1984; *Luo*, 1994; *McDonald*, 1998]. While a TC moves northwestward due to mean flow steering and beta draft, it emits Rossby wave energy southeastward, forming a synoptic-scale wave train with alternating anticyclonic and cyclonic vorticity perturbations [*Holland*, 1995; *Carr and Elsberry*, 1994, 1995]. The second process is associated with energy accumulation of easterly waves in a confluence region where the monsoon westerly wind meets the easterly trade wind. The scale contraction of the easterly waves could lead to the accumulation of kinetic energy in a critical longitude where the mean flow converges [*Kuo et al.*, 2001]. This energy accumulation could lead to the successive development of tropical storms in the monsoon confluence region. It is similar to the energy accumulation mechanism previously used to explain Atlantic cyclogenesis from preexisting easterly waves by *Shapiro* [1977]. In addition, the cyclogenesis may result from the wave-mean flow interaction [*Ferreira and Schubert*, 1997; *Zehnder et al.*, 1999; *Molinari et al.*, 2000], synoptic-scale wave trains [*Lau and Lau*, 1990; *Chang et al.*, 1996], or a mixed Rossby-gravity wave packet [*Dickinson and Molinari*, 2002]. *Sobel and Bretherton* [1999] analyzed the energy flux convergence in the WNP and found that the wave accumulation may operate either on waves coming from outside of the region or in situ, in particular, mature TCs.

[5] The TC energy dispersion mechanism was suggested previously with indirect (e.g., ECMWF analysis) and limited observational data sources. For instance, *Frank* [1982] and *Briegel and Frank* [1997] suggested the role of TC energy dispersion based on the number and location of pre-existing TCs relative to the location of new storms at time of cyclogenesis. These analyses did not provide the detailed structure and evolution characteristics of Rossby wave train induced by TC energy dispersion, neither a relationship between the wave train and cyclogenesis. The role of easterly waves on cyclogenesis was demonstrated in a barotropic model [*Kuo et al.*, 2001], which also requires support from direct measurements. Recent satellite products provide a great opportunity to reveal synoptic-scale wave structures prior to TC formation. Using these satellite data, we will first display atmospheric wave structure and propagation characteristics prior to TC formation. We will then

[1]Naval Research Laboratory, Monterey, California, USA


0094-8276/03/2003GL018556$05.00

use a hurricane model to simulate the two cyclogenesis processes.

## 2. Synoptic Wave Structures Prior to Cyclogenesis Revealed From Direct Satellite Measurements

[6] To document the cyclogenesis processes over the WNP, we first conducted an observational study by analyzing high-resolution ($0.25^\circ \times 0.25^\circ$) daily data from NASA Tropical Rainfall Measurement Mission (TRMM) Microwave Image (TMI) and QuikSCAT Level 3 products. The QuikSCAT data provide surface wind vector fields and the TMI data provide precipitation and surface wind speed fields. An optimal interpolation scheme was utilized to fill the gaps between these two data sets. A band-pass (3–8 day) filter was then applied in order to extract the synoptic-scale signals.

[7] We focus on the cyclogenesis processes associated with the TC Rossby wave energy dispersion and the easterly wave forcing. During the summer of 2000 and 2001, there were a total of 34 cyclogenesis cases (in which the vortex reached tropical storm strength). Among them, 7 and 6 are related to the easterly wave forcing and the TC energy dispersion mechanisms, respectively.

[8] Figure 1 shows a scenario of the Rossby wave energy dispersion. It illustrates the time sequence of synoptic-scale wind patterns associated with a named TC Jelawat, which formed on 1 August 2000. During the first few days, Jelawat did not excite any significant Rossby wave train in its wake due to its relatively weak intensity. As it intensified on its northwestward route, a Rossby wave train developed in its wake. A northwest-southeast oriented wave train was clearly seen on August 6, and it had a typical zonal wavelength of 2500 km. A significant feature of this wave train was its rather large meridional length scale as compared with its zonal length scale. Based on non-divergent barotropic vorticity dynamics, we argue that this feature is essential for the eastward energy propagation. This is analyzed in the following.

[9] Denote $k$ and $l$ as the zonal and meridional wave number, the zonal and meridional components of the group velocity of the Rossby wave can be represented as

$$C_{gx} = \frac{\beta(k^2 - l^2)}{(k^2 + l^2)^2}, \tag{1}$$

$$C_{gy} = \frac{2\beta kl}{(k^2 + l^2)^2}, \tag{2}$$

where $\beta$ is the meridional gradient of the Coriolis parameter.

[10] The equations above indicate that when the meridional wavelength exceeds the corresponding zonal wavelength (i.e., $k^2 > l^2$), wave energy propagates eastward as the zonal group velocity is positive. The opposite signs of $k$ and $l$ (due to the northwestward phase propagation) imply that the Rossby wave energy also propagates southward. In combination, the energy associated with the Rossby wave train propagates southeastward.

[11] A remarkable feature associated with the aforementioned Rossby wave train is its scale contraction, in particular the meridional scale. This is evident from August 7 to 9 as shown in Figure 1. Following this scale contraction, a new TC named Ewiniar formed in the positive vorticity region of the Jelawat's wave train on 9 August 2000. This analysis of the satellite data presents convincing evidences for the existence of Rossby wave trains associated with an existing TC and the formation of a subsequent TC in the wake of the pre-existing TC.

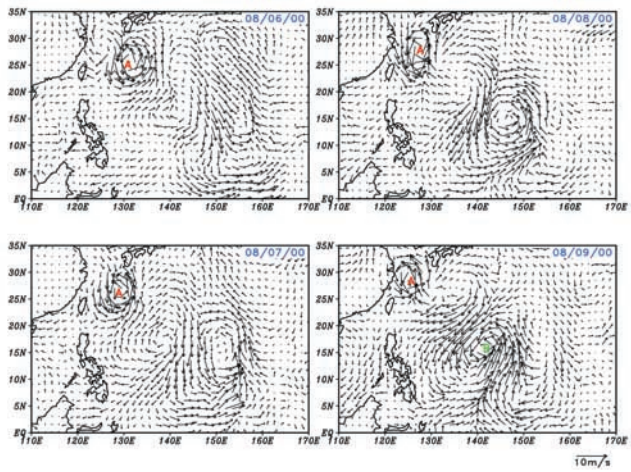


**Figure 1.** Time evolution of Rossby wave train associated with the energy dispersion of TC Jelawat as seen from the QuikSCAT surface wind observation. "A" represents the center location of TC Jelawat that formed on 1 August 2000. "B" represents the center location of a new TC named Ewiniar that was generated on 9 August 2000 in the wake of the Rossby wave train of Jelawat.

[12] Not all TCs have a Rossby wave train in their wakes. We notice that the wave train is more frequently observed for more intense TCs. The excitation of the wave train also depends on the background wind. For strong TCs (central pressure below 960 mb), the Rossby wave trains are only evident west of 160°E where the mean easterly flow is relatively weak.

[13] The second tropical cyclogenesis process is associated with the effect of pre-existing easterly waves. For readers' familiarity, we use the same TC Jelawat as an example. The westward propagation of the easterly wave in this case is revealed in Figure 2 by the time-longitude diagram of the perturbation energy and precipitation fields along the latitude where Typhoon Jelawat formed (22°N). The wave signals can be traced back eastward to the dateline 4–5 days prior to Jelawat's formation. Both fields exhibit clear wave propagation signals at a speed of approximately 5° longitudes per day prior to the formation of Jelawat. We found that the simultaneous westward propagation of the perturbation energy and precipitation is a robust precursor of the second cyclogenesis scenario.

[14] Figures 1 and 2 provide the observational support of roles the TC energy dispersion and the pre-existing easterly waves play on tropical cyclogenesis in the WNP. In both scenarios, synoptic wave conditions a few days prior to the TC formation provide a possible precursor for real-time cyclogenesis forecast. A challenge remains whether we can simulate the subsequent cyclone development in a

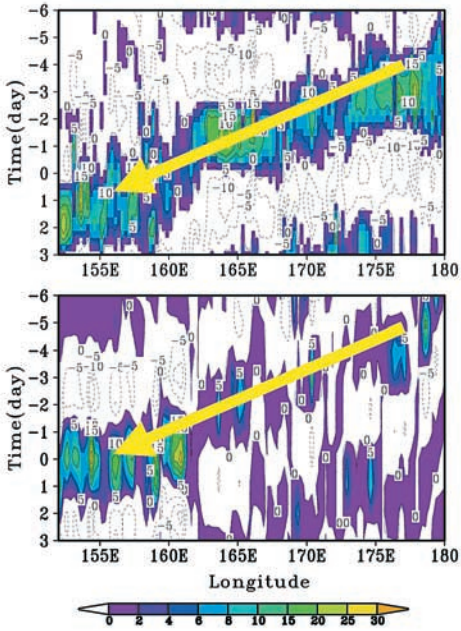


**Figure 2.** Time-longitude profiles of the surface kinetic energy $\frac{1}{2}(u^2 + v^2)$ (upper panel, units: $m^2s^{-2}$) and precipitation rate (lower panel, units: $mmday^{-1}$) along 22°N. The horizontal axis is longitude and the vertical axis is time in days. Typhoon Jelawat formed at 153°E, 22°N on 1 August 2000 (corresponding to day 0). Both panels show clear westward-propagating signals prior to the birth of Jelawat.

numerical weather prediction model given a synoptic wave structure similar to the observed as the initial condition.

## 3. Simulation of Cyclogenesis in a 3D Model

[15] Motivated by the satellite data analyses on the roles of the easterly wave and TC energy dispersion on subsequent TC formation, we further simulate these two cyclogenesis processes in a hurricane model. The model used here is the TCM3 model developed by *Wang* [2001]. The model is capable of simulating the structure of TC spiral rainband and eye wall. It has been used for study of maximum potential TC intensity [*Holland*, 1997] and vortex Rossby waves [*Wang*, 2002]. We modified the model so that a time-independent basic flow can be specified. The perturbation governing equations are fully nonlinear.

[16] Our first attempt is to simulate the cyclogenesis associated with the Rossby wave energy dispersion of a preexisting TC. In this experiment, a mature TC with its well-developed Rossby wave train is specified initially. Two different convective heating treatments, one with an explicit convective heating scheme and the other with a parameterized mass-flux scheme [*Tiedtke*, 1989], were used. In both cases, the TC formation was realistically reproduced in the presence of the idealized basic flow that is similar to the observed summer mean flow in the WNP. Figure 3 shows the simulation with the explicit convective heating scheme. A new TC (with minimum central pressure of 975 hPa) forms in the wake of a pre-existing TC at day 5. The simulated TC has realistic dynamic and thermal structures. For instance, the maximum tangential wind appears near the core region of TC at a radius of about 60 km, typically observed. A warm core appears in the center of the vortex with the maximum amplitude in the upper troposphere. A spiral rain band rotates around the TC center.

[17] The summer mean flow plays a critical role in organizing the TC-scale convection. A sensitivity experiment was conducted in which the summer mean flow was removed. No TC-like vortex was generated in the Rossby wave train, suggesting the importance of the wave-mean flow interaction.

[18] Next, we simulate the cyclogenesis process associated with the easterly wave forcing. Studies such as *Kuo et al.* [2001] have investigated the easterly wave energy accumulation using a non-divergent barotropic model in which critical roles of convective heating were ignored. Observations, however, show that latent heat release in deep convection is a major heat source for tropical storm formation. An issue arises as to how the interaction of the convective heating and the synoptic-scale waves leads to the formation of TCs.

[19] Following *Kuo et al.* [2001], an easterly wave source is specified in the eastern boundary (centered at 18°N) of the model domain and is confined within 10-degree longitude distance away from the boundary in the lower troposphere. The easterly wave forcing has a Rossby wave structure with a wavelength of 2500 km. An idealized zonal confluence flow is specified as the basic state. Both the phase and energy of the forced waves propagate westward in the presence of the basic-state easterly to the east of the confluence zone. The perturbation energy is accumulated near the confluence zone owing to scale contraction by the

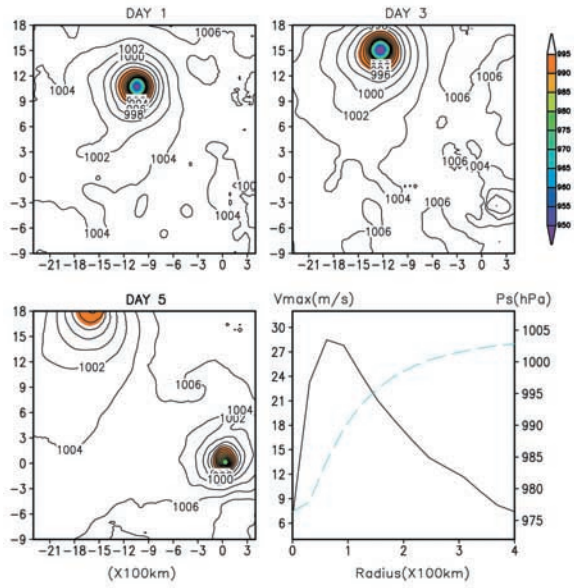


**Figure 3.** Evolution of the surface pressure at day 1, 3, and 5 simulated by a hurricane model. A new TC is generated in the wake of a pre-existing TC at day 5. The horizontal and vertical axes represent distance in x and y direction (units: 100 km). The lower-right panel shows the radial profile of the surface pressure (dashed line, *mb*) and tangential wind (solid line, $ms^{-1}$) of the new TC at day 5.

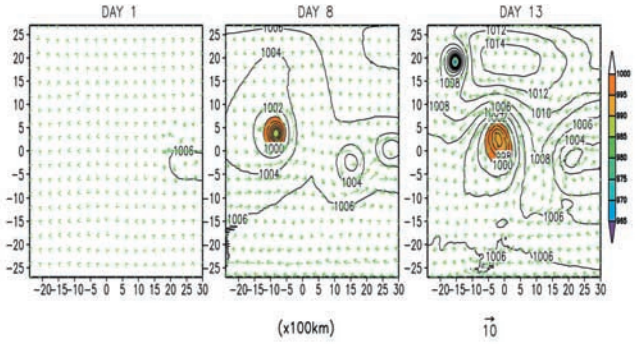


**Figure 4.** Evolution of the surface pressure and wind fields at day 1, 8, and 13 simulated by a hurricane model under an idealized monsoon confluence flow. The first new TC is generated in the confluence zone at day 7 and then moves northwestward. The second TC is generated at day 13. The horizontal and vertical axes represent distance from the monsoon confluence zone.

confluent background flow and nonlinear dynamics that sharpens potential vorticity (PV) gradients.

[20] The energy accumulation of the easterly waves leads to growth of positive PV in the monsoon confluence zone. The convection-circulation feedback further enhances the development of the PV disturbance. At day 8, a well-organized TC forms, which has a minimum central pressure of 980 hPa (Figure 4). Due to the continuous easterly wave forcing from the eastern boundary, a second vortex is generated a few days later in the same confluence region, as the first cyclone intensifies and moves away. The numerical experiments demonstrate the potential capability of predicting TC formation in real time with use of the satellite observations.

## 4. Conclusion

[21] Using the TRMM TMI and QuikSCAT data from satellite, we have documented two important cyclogenesis processes associated with TC formation in the WNP during 2000 and 2001: Rossby wave energy dispersion from a preexisting TC and the easterly wave forcing mechanism.

[22] Although past studies have identified these mechanisms based on analysis fields, here the structure of a Rossby wave train associated with TC energy dispersion is revealed by direct satellite measurements. The wave train has alternating anticyclonic and cyclonic circulations, oriented in a northwest-southeast direction with a preferred wavelength of 2000–3000 km. Our analysis shows that a new TC can form in the cyclonic vorticity region of the wave train through a meridional scale contraction of the Rossby wave disturbance. Note that not all TCs have a Rossby wave train in their wakes. The occurrence of the Rossby wave train depends on TC intensity and background mean flows.

[23] Cyclogenesis cases associated with easterly waves were identified by detecting westward propagation signals passing the location of the cyclone center in both perturbation kinetic energy and precipitation fields. These wave signals may be traced back 4–5 days prior to cyclogenesis, thus can be served as a precursor for real-time cyclogenesis forecast.

[24] Numerical model experiments are conducted to simulate these two cyclogenesis processes. The results demonstrate that a new TC with realistic dynamic and thermodynamic structures can form either in the wake of a mature TC due to Rossby wave energy dispersion or in the monsoon confluence zone due to the energy accumulation of easterly waves.

[25] The success of the numerical experiments on TC formation lends hopes for real-time operational dynamic forecast. A dynamic model for tropical cyclogenesis forecast is under development by our group. We plan to use the newest satellite-derived products such as Advanced Microwave Sounding Units (AMSU) data that provide 3-dimensional structure and temporal evolution of atmospheric temperature and moisture fields over the oceans. These products together with other satellite data such as the QuikSCAT wind products may provide synoptic wave structures prior to the formation of a tropical cyclone. Through proper insertion of these data into the numerical model such as three-dimensional variational method (3D VAR), we hope to achieve breakthrough in real-time prediction of TC formation.

[26] **Acknowledgments.** We thank Drs. Yuqing Wang and Yongti Zhu for valuable discussions. This work was supported by NSF Grant ATM01-19490 and ONR Grants N000140210532 and N000140310739. International Pacific Research Center is partially sponsored by the Frontier Research System for Global Change. This is SOEST contribution number 6297 and IPRC contribution number 245.

## References

Anthes, R. A., Tropical cyclone: Their evolution, structure and effects. *Meteorol. Mongr.* No. 41, *Am. Meteorol. Soc*., 208 pp., 1982.

Briegel, L. M., and W. M. Frank, Large-scale influences on tropical cyclogenesis in the western North Pacific, *Mon. Wea. Rev.*, *125*, 1397–1413, 1997.

Carr, L. E., and R. L. Elsberry, Systematic and integrated approach to tropical cyclone track forecasting. Part 1: Approach overview and description of meteorological basis, *Technical Report,* Naval Postgraduate School, NPS-MR-94-002, 273 pp., 1994.

Carr, L. E., and R. L. Elsberry, Monsoonal interactions leading to sadden tropical cyclone track changes, *Mon. Wea. Rev.*, *123*, 265–289, 1995.

Chang, C.-P., J.-M. Chen, P. A. Harr, and L. E. Carr, Northwestward-propagating wave patterns over the tropical western north Pacific during summer, *Mon. Wea. Rev.*, *124*, 2245–2266, 1996.

Davidson, N. E., and H. H. Hendon, Downstream development in the southern hemisphere monsoon during FGGE/WMONEX, *Mon. Wea. Rev.*, *117*, 1458–1470, 1989.

Dickinson, M., and J. Molinari, Mixed Rossby-gravity waves and western Pacific tropical cyclogenesis, Part I: Synoptic evolution, *J. Atmos. Sci.*, *59*, 2183–2196, 2002.

Ferreira, R. N., and W. H. Schubert, Barotropic aspects of ITCZ breakdown, *J. Atmos. Sci.*, *54*, 261–285, 1997.

Flierl, G. R., Rossby wave radiation from a strongly nonlinear warm eddy, *J. Phys. Oceanogr.*, *14*, 47–58, 1984.

Frank, W. M., Large-scale characteristics of tropical cyclones, *Mon. Wea. Rev.*, *110*, 572–586, 1982.

Gray, W. M., Global view of the origin of tropical disturbances and storms, *Mon. Wea. Rev.*, *96*, 669–700, 1968.

Holland, G. J., Scale interaction in the western Pacific monsoon, *Meteorol. Atmos. Phys.*, *56*, 57–79, 1995.

Holland, G. J., The maximum potential intensity of tropical cyclones, *J. Atmos. Sci.*, *54*, 2519–2541, 1997.

Kuo, H.-C., J.-H. Chen, R. T. Williams, and C.-P. Chang, Rossby wave in zonally opposing mean flow: Behavior in northwest Pacific summer monsoon, *J. Atmos. Sci.*, *58*, 1035–1050, 2001.

Kurihara, Y., M. A. Bender, R. E. Tuleya, and R. J. Ross, Improvements in the GFDL hurricane prediction system, *Mon. Wea. Rev.*, *123*, 2791–2801, 1995.

Lau, K.-H., and N.-C. Lau, Observed structure and propagation characteristics of tropical summertime synoptic scale disturbances, *Mon. Wea. Rev.*, *118*, 1888–1913, 1990.

Luo, Z., Effect of energy dispersion on the structure and motion of tropical cyclone, *Acta Meteorol. Sinica*, *8*, 51–59, 1994.

McDonald, N. R., The decay of cyclonic eddies by Rossby wave radiation, *J. Fluid Mech.*, *361*, 237–252, 1998.

Molinari, J., D. Vollaro, S. Skubis, and M. Dickinson, Origin and mechanism of eastern Pacific tropical cyclogenesis: A case study, *Mon. Wea. Rev.*, *128*, 125–139, 2000.

Ritchie, E. A., and G. J. Holland, Scale interactions during the formation of typhoon Irving, *Mon. Wea. Rev.*, *125*, 1377–1396, 1997.

Ritchie, E. A., and G. J. Holland, Large-scale patterns associated with tropical cyclogenesis in the western Pacific, *Mon. Wea. Rev.*, *127*, 2027–2043, 1999.

Shapiro, L. J., Tropical storm formation from easterly waves: A criterion for development, *J. Atmos. Sci.*, *34*, 1007–1021, 1977.

Sobel, A. H., and C. S. Bretherton, Development of synoptic-scale disturbances over the summertime tropical northwest Pacific, *J. Atmos. Sci.*, *56*, 3106–3127, 1999.

Tiedtke, M., A comprehensive mass flux scheme for cumulus parameterization in large-scale models, *Mon. Wea. Rev.*, *117*, 1779–1800, 1989.

Wang, Y., An explicit simulation of tropical cyclones with a triply nested movable mesh primitive equation model: TCM3. Part I: Model description and control experiment, *Mon. Wea. Rev.*, *129*, 1370–1394, 2001.

Wang, Y., Vortex Rossby waves in a numerically simulated tropical cyclone. Part I: Overall structure, potential vorticity and kinetic energy budgets, *J. Atmos. Sci.*, *59*, 1213–1238, 2002.

Zehnder, J. A., D. Powell, and D. Ropp, The interaction of easterly waves, orography and the ITCZ in the genesis of eastern Pacific tropical cyclones, *Mon. Wea. Rev.*, *127*, 1566–1585, 1999.

T. Li, IPRC and Department of Meteorology, University of Hawaii, 2525 Correa Rd., Honolulu, HI 96822, USA. (timli@hawaii.edu)

X. Ge, B. Fu, and B. Wang, Department of Meteorology, University of Hawaii, 2525 Correa Rd., Honolulu, HI 96822, USA.

M. Peng, Naval Research Lab., 7 Grace Hopper Ave., Monterey, CA 93943, USA.